

# Guaranteeing Control Requirements via Reward Shaping in Reinforcement Learning

Francesco De Lellis *Member, IEEE*, Marco Coraggio *Member, IEEE*, Giovanni Russo *Senior Member, IEEE*,  
Mirco Musolesi *Member, IEEE*, Mario di Bernardo *Fellow, IEEE*

**Abstract**—In addressing control problems such as regulation and tracking through reinforcement learning, it is often required to guarantee that the acquired policy meets essential performance and stability criteria such as a desired settling time and steady-state error prior to deployment. Motivated by this necessity, we present a set of results and a systematic reward shaping procedure that (i) ensures the optimal policy generates trajectories that align with specified control requirements and (ii) allows to assess whether any given policy satisfies them. We validate our approach through comprehensive numerical experiments conducted in two representative environments from OpenAI Gym: the Inverted Pendulum swing-up problem and the Lunar Lander. Utilizing both tabular and deep reinforcement learning methods, our experiments consistently affirm the efficacy of our proposed framework, highlighting its effectiveness in ensuring policy adherence to the prescribed control requirements.

**Index Terms**—Learning-Based Control, Reward Shaping, Policy validation, Deep Reinforcement Learning, Computational Control

## I. INTRODUCTION

The paradigm of using reinforcement learning (RL) for control system design has gained substantial traction due to its ability to autonomously learn policies that effectively address complex control problems, relying solely on data and employing a reward maximization process. This approach finds diverse applications, spanning from attitude control [1] and wind farm management [2] to autonomous car-driving [3] and the regulation of plasma using high-fidelity simulators [4]. However, a significant challenge in this domain revolves around ensuring that the learned control policy demonstrates

the desired closed-loop performance and steady-state error, posing a crucial open question in control system design.

It is often argued that accurate knowledge of system dynamics is necessary to provide analytical guarantees of stability and performance, which is crucial for industrial applications [5], [6]. In fact, in this paper, we introduce a set of analytical results and a constructive procedure for shaping the reward function of approaches based on reinforcement learning (tabular and function approximation methods that rely on deep learning). The goal is to derive a learned policy which is obtained without the use of a mathematical model of the system dynamics, able to verifiably meet predetermined control requirements in terms of desired settling time and steady-state error.

In the Literature, *reward shaping*, consisting of modifying the reward function in order to improve learning or control performance, has mostly been used to increase sample efficiency [7]–[9], rather than provide guarantees on the learned policy. An early example was presented in [7], where an agent was trained to ride a bicycle exploiting a reward shaping mechanism. More recently, reduced sample complexity was demonstrated in [9] for a modified Upper Confidence Bound algorithm using shaped rewards. In [8], it was shown that adding a function of the state to the reward keeps the optimal policy unchanged if and only if the function is potential-based. A method to select potential-based functions is presented and validated analytically in [10], requiring knowledge of an appropriate Lyapunov function, to guarantee convergence to a state under the optimal policy. While this result can be used to solve regulation problems, it does not ensure a specific settling time. Moreover, finding a Lyapunov function is often cumbersome for many real-world problems.

When guarantees are given on reinforcement learning control [6], they are typically provided in terms of reachability of certain subsets of the state space [11], [12], or in terms of *safety* during learning and/or for the learned policy. Namely, in [11], RL is used to select a control law among a set of candidates, using Lyapunov functions to ensure a system enters a goal region with unitary probability, under certain conditions on the controllers. In [12], a partially known system model is used to improve a safe starting policy through RL, avoiding actions that bring the system out of the basin of attraction of a desired equilibrium. Both approaches [11], [12] do not provide guarantees on the time required to reach the desired regions. Safety for RL control has been extensively explored in the Literature using various frameworks, such as *constrained Markov decision processes* [13], “shields” [14], *control barrier*

This work was in part supported by the Research Project “SHARESPACE” funded by the European Union (EU HORIZON-CL4-2022- HUMAN-01-14. SHARESPACE. GA 101092889 - <http://sharespace.eu>) and by the Research Project PRIN 2022 “Machine-learning based control of complex multi-agent systems for search and rescue operations in natural disasters (MENTOR)” funded by the Italian Ministry of University and Research (2023–2025).

F. De Lellis is with the Department of Electrical Engineering and Information Technology, University of Naples Federico II, Naples, Italy (e-mail: francesco.delellis@unina.it).

M. Coraggio is with the Scuola Superiore Meridionale, School for Advanced Studies, Naples, Italy (e-mail: marco.coraggio@unina.it).

G. Russo is with the Department of Computer and Electrical Engineering & Applied Mathematics, University of Salerno, DIEM, Salerno, Italy (e-mail: giovorusso@unisa.it).

M. Musolesi is with the Department of Computer Science, University College London, U.K. and the Department of Informatics - Science and Engineering, University of Bologna, Bologna, Italy (e-mail: m.musolesi@ucl.ac.uk).

M. di Bernardo is with the Department of Electrical Engineering and Information Technology, University of Naples Federico II, Naples, Italy, and with the Scuola Superiore Meridionale, School for Advanced Studies, Naples, Italy (e-mail: mario.dibernardo@unina.it).

functions [15], and a combination of Model Predictive Control and RL [16]. Although these techniques ensure avoidance of unsafe subsets of the state space, they generally do not provide guarantees on reaching a specific goal region or on control performance metrics, such as settling time.

The problem of synthesizing rewards for control tasks is also the subject of *inverse optimal control* (IOC) [17], focusing on estimating the rewards associated to given observations of states and control inputs, assuming closed-loop stability and/or policy optimality. Initially aimed at determining control functions producing observed outputs [18], IOC has since been connected to reinforcement learning [19], applied in nonlinear, stochastic environments [20], and its framework has been used to investigate the cost design problem [21]. However, to the best of our knowledge, IOC has not been used specifically to design reward functions that, when optimized for, can guarantee specific control performance.

Given a regulation or tracking problem with predetermined stability and performance requirements on steady-state error and settling time, we advance the state of the art as follows.

- 1) We introduce a model-free sufficient condition on the discounted return associated to a trajectory to determine if it is *acceptable* (i.e., it satisfies the control requirements).
- 2) We give a sufficient condition to assess whether a learned policy leads to an acceptable closed-loop trajectory.
- 3) We provide a procedure to shape the reward function so that the above conditions can be applied on a system of interest and that the optimal policy is acceptable.
- 4) We successfully validate the approach through two representative control problems from OpenAI Gym [22]: the stabilization of an inverted pendulum [23], and performing landing in the Lunar Lander environment [24].

For reproducibility, the code is available on GitHub [25].

The rest of the paper is organized as follows. In Section II, we formalize the problem of constructing a reward function for learning-based control. The main results of our approach are then presented in Section III and validated via numerical simulations on two representative application examples in Section IV. Concluding remarks are given in Section V.

## II. PROBLEM STATEMENT

### A. Problem set-up

We consider a discrete time dynamical system of the form

$$x_{k+1} = f(x_k, u_k), \quad x_0 = \tilde{x}_0, \quad (1)$$

where  $k \in \mathbb{N}_{\geq 0}$  is discrete time,  $x_k \in \mathcal{X}$  is the *state* at time  $k$ ,  $\mathcal{X}$  is the *state space*,  $\tilde{x}_0 \in \mathcal{X}$  is an *initial condition*,  $u_k \in \mathcal{U}$  is the *control input* (or *action*) at time  $k$ ,  $\mathcal{U}$  is the *set of feasible inputs*, and  $f: \mathcal{X} \times \mathcal{U} \rightarrow \mathcal{X}$  is the *system dynamics*.

Furthermore, we let  $\pi: \mathcal{X} \rightarrow \mathcal{U}$  be a *control policy*, and let  $u_k = \pi(x_k)$ . Let also  $\mathcal{X}^\infty := \mathcal{X} \times \dots \times \mathcal{X}$ , with the Cartesian product being applied an infinite number of times. We denote by  $\phi^\pi(\tilde{x}_0) \in \mathcal{X}^\infty$  the *trajectory* obtained by applying policy  $\pi$  to system (1) starting from  $\tilde{x}_0$  as initial state.

We are interested in finding a policy such that the trajectory generated by it (starting from a given  $\tilde{x}_0$ ) reaches a desired *goal region*  $\mathcal{G} \subset \mathcal{X}$  before some *desired settling time*  $k_s \in \mathbb{N}_{>0}$

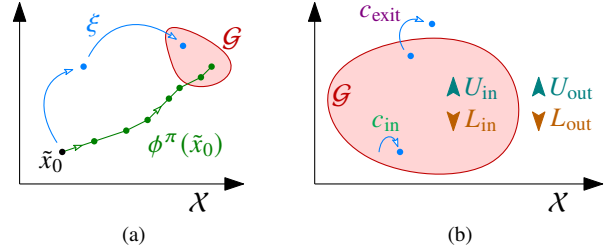


Fig. 1. (a): A state-space sequence  $\xi$ , a trajectory  $\phi^\pi(\tilde{x}_0)$ , and a goal region  $\mathcal{G}$  (see Section II); while a state-space sequence is simply a sequence of points in the state space  $\mathcal{X}$ , a trajectory is generated by applying a policy to the dynamics in (1). (b): Terms of the reward structure in Assumption III.1.

and remains in this region for at least a *desired permanence time*  $k_p \in \mathbb{N}_{>0}$  (see Definition II.3 below for the rigorous statements). For example,  $\mathcal{G}$  could be an arbitrarily small neighborhood of a reference state, with a radius equal to the admitted steady-state error. In our main results, we assume  $\mathcal{G}$ ,  $k_s$ ,  $k_p$  are given; nonetheless, in Section III (see Remark III.8), we will observe that  $k_p$  can be arbitrarily large, and in Proposition A.1 (in the Appendix), we give a criterion to assess the feasibility of the settling time constraint when limited knowledge about the system to control is available.

### B. Acceptable state-space sequences

We will now introduce concepts that will be used for the formalization of the proposed approach.

**Definition II.1** (State-space sequences). A state-space sequence is a sequence  $\xi = (x_k)_{k \in [0, +\infty)} \in \mathcal{X}^\infty$ .

Note that all trajectories are state-space sequences, but the converse is not true. As a matter of fact, given a state-space sequence  $\xi$  with  $x_0 = \tilde{x}_0 \in \mathcal{X}$ , there is no guarantee that there exists a policy  $\pi$  such that  $\phi^\pi(\tilde{x}_0) = \xi$ . A graphical representation of these concepts is reported in Figure 1a.

**Definition II.2** (First exit instant). The first exit instant  $k_{\text{exit}}(\xi) \in \mathbb{N}_{>0}$  of a state-space sequence  $\xi = (x_k)_{k \in [0, +\infty)}$  is the smallest time instant such that, in  $\xi$ , we have  $x_{k_{\text{exit}}(\xi)-1} \in \mathcal{G}$  and  $x_{k_{\text{exit}}(\xi)} \notin \mathcal{G}$ ; if this condition never occurs in  $\xi$ , we set  $k_{\text{exit}}(\xi) = \infty$ .

Next, we define the set of acceptable state-space sequences, trajectories, and policies, i.e., those that satisfy the performance and steady-state specifications.

**Definition II.3** (Acceptable state-space sequences, trajectories and policies). Given the desired goal region  $\mathcal{G}$ , the desired settling time  $k_s$ , and the desired permanence time  $k_p$ , a state-space sequence  $\xi = (x_0, x_1, x_2, \dots)$  or equivalently a trajectory  $\phi^\pi(\tilde{x}_0) = (\tilde{x}_0, x_1, x_2, \dots)$  are acceptable if

- 1)  $\exists k \leq k_s : x_k \in \mathcal{G}$  (i.e., the state is in  $\mathcal{G}$  not later than time  $k_s$ );
- 2)  $k_{\text{exit}}(\xi) > k_p$  (i.e., the state does not exit  $\mathcal{G}$  before time  $k_p$ , included).

A policy  $\pi$  is acceptable from  $\tilde{x}_0$  if  $\phi^\pi(\tilde{x}_0)$  is acceptable.

It can be immediately verified that there exists at least one acceptable state-space sequence provided that  $\mathcal{G} \neq \emptyset$ . Indeed,

this state-space sequence is  $\xi = (x_0, x_1, \dots)$  with  $x_k \in \mathcal{G}$  for all  $k$ , which can be verified to be acceptable by checking the two conditions in Definition II.3.

### C. Using reinforcement learning to find acceptable control policies

Following [26], [27], we employ a reinforcement learning solution to automatically identify an acceptable policy for a given initial condition  $\tilde{x}_0$ , and to do so without the need of knowing the dynamics  $f$ . Namely, let  $r : \mathcal{X} \times \mathcal{X} \times \mathcal{U} \rightarrow \mathbb{R}$  be a *reward function*, so that  $r(x', x, u)$  is the reward obtained by the agent when taking action  $u$  in state  $x$  and arriving at the new state  $x'$  at the next time instant. Let also  $J^\pi : \mathcal{X}^\infty \rightarrow \mathbb{R}$  be the (*discounted*) *return function* defined as

$$J^\pi(\xi) := \sum_{k=1}^{\infty} \gamma^{k-1} r(x_k, x_{k-1}, u_{k-1}), \quad (2)$$

where  $\xi \in \mathcal{X}^\infty$  is a state-space sequence,  $u_k = \pi(x_k)$ , and  $\gamma \in [0, 1]$  is a given *discount factor*.<sup>1</sup> To find an acceptable policy, we set the following optimization problem and solve it via reinforcement learning:

$$\max_{\pi} J^\pi(\phi^\pi(\tilde{x}_0)), \quad (3a)$$

$$\text{s.t. } x_{k+1} = f(x_k, u_k), \quad k \in \{0, 1, 2, \dots\}, \quad (3b)$$

$$u_k = \pi(x_k), \quad k \in \{0, 1, 2, \dots\}, \quad (3c)$$

$$x_0 = \tilde{x}_0 \in \mathcal{X}. \quad (3d)$$

Thus, the problem we aim to solve can be stated as follows.

#### Problem II.4. Shape the reward function $r$ so that:

- (i) it is possible to determine that a trajectory  $\phi^\pi(\tilde{x}_0)$  is acceptable by assessing the value of  $J^\pi(\phi^\pi(\tilde{x}_0))$ ;
- (ii) an acceptable policy from  $\tilde{x}_0$  (provided it exists) can be found by solving (3).

## III. MAIN RESULTS

In Section III-A, we relate acceptable state-space sequences and their return (solving point (i) in Problem II.4), in Section III-C, we embed the theory in a constructive procedure to shape rewards, in Section III-D, we give analogous results for trajectories, and finally in Section III-E, we show that acceptable policies can be found using reinforcement learning algorithms. The assumptions we make and how they are related are schematically summarized in Figure 2.

### A. Assessing acceptable state-space sequences

We start by defining the structure of the shaped reward.

**Assumption III.1** (Reward structure). *The reward function can be written as*

$$r(x', x, u) = r^b(x', x, u) + r^c(x', x), \quad (4)$$

<sup>1</sup>According to this formulation, it is possible to evaluate  $J^\pi$  on a state-space sequence that is not a trajectory (which is needed for the theoretical results presented in Section III); in this case, even though the value of the states are not generated following policy  $\pi$ , in general it is still necessary to specify  $\pi$  to obtain the values of the inputs  $u_k$  used for the computation of the reward  $r$ . When  $J^\pi$  is evaluated on a trajectory, e.g.,  $J^{\pi_1}(\phi^{\pi_2})$ , we will only consider the case in which  $\pi_1 = \pi_2$ .

where

- $r^b : \mathcal{X} \times \mathcal{X} \times \mathcal{U} \rightarrow \mathbb{R}$  is a bounded reward term, i.e., such that there exist finite  $U_{\text{out}}, U_{\text{in}}, L_{\text{out}}, L_{\text{in}} \in \mathbb{R}$  such that

$$\sup_{x' \in \mathcal{X} \setminus \mathcal{G}, x \in \mathcal{X}, u \in \mathcal{U}} r^b(x', x, u) \leq U_{\text{out}}, \quad (5a)$$

$$\sup_{x' \in \mathcal{G}, x \in \mathcal{X}, u \in \mathcal{U}} r^b(x', x, u) \leq U_{\text{in}}, \quad (5b)$$

$$\inf_{x' \in \mathcal{X} \setminus \mathcal{G}, x \in \mathcal{X}, u \in \mathcal{U}} r^b(x', x, u) \geq L_{\text{out}}, \quad (5c)$$

$$\inf_{x' \in \mathcal{G}, x \in \mathcal{X}, u \in \mathcal{U}} r^b(x', x, u) \geq L_{\text{in}}. \quad (5d)$$

- $r^c : \mathcal{X} \times \mathcal{X} \rightarrow \mathbb{R}$  is a correction term given by

$$r^c(x', x) = \begin{cases} r_{\text{in}}^c, & \text{if } x' \in \mathcal{G}, \\ r_{\text{exit}}^c, & \text{if } x \in \mathcal{G} \text{ and } x' \notin \mathcal{G}, \\ 0, & \text{otherwise,} \end{cases} \quad (6)$$

with  $r_{\text{in}}^c, r_{\text{exit}}^c \in \mathbb{R}$ . Moreover, it holds that

$$r_{\text{in}}^c \geq U_{\text{out}} - L_{\text{in}}. \quad (7)$$

In practice,  $r_{\text{in}}^c$  will typically be a positive reward for being inside the goal region, while  $r_{\text{exit}}^c$  will normally be a negative reward for having left the goal region—please, refer to Figure 1b for a diagrammatic representation.

**Remark III.2** (Generality of Assumption III.1). *Assumption III.1 is not too restrictive. Indeed, if one wants to use a preexisting reward, it is only required it is bounded (see (5)). It can then be shaped by adding the correction term  $r^c$  to it.*

We also define the differences

$$\Delta_{\text{in}} := U_{\text{in}} - L_{\text{in}} \geq 0, \quad (8a)$$

$$\Delta_{\text{out}} := U_{\text{out}} - L_{\text{out}} \geq 0. \quad (8b)$$

To assess properties of state-space sequences, trajectories, and policies from their associated return, we define the *return threshold*  $\sigma \in \mathbb{R}$  and introduce the following definition.

**Definition III.3** (High-return state-space sequences, trajectories and policies). *A state-space sequence  $\xi$  is high-return if  $J^\pi(\xi) > \sigma$  for any policy  $\pi$ . A trajectory  $\phi^\pi(\tilde{x}_0)$  is high-return if  $J^\pi(\phi^\pi(\tilde{x}_0)) > \sigma$ . A policy  $\pi$  is high-return from  $\tilde{x}_0$  if  $\phi^\pi(\tilde{x}_0)$  is high-return.*

Of the quantities introduced so far, those that we assume to be given (i.e., fixed) are  $\mathcal{G}, k_s, k_p, \gamma, U_{\text{in}}, U_{\text{out}}, L_{\text{in}}, L_{\text{out}}$ ; conversely, the quantities to be designed are  $\sigma, r_{\text{in}}^c, r_{\text{exit}}^c$ .

Next, we introduce an assumption on the correction terms in the reward.

**Assumption III.4.** *Assume that*

$$\sigma \geq \frac{U_{\text{out}}}{1 - \gamma}, \quad (9)$$

and, given the desired settling time  $k_s$  and the desired permanence time  $k_p$ , assume that

$$r_{\text{in}}^c \leq -U_{\text{in}} - U_{\text{out}} \frac{1 - \gamma^{k_s}}{\gamma^{k_s}} + \sigma \frac{1 - \gamma}{\gamma^{k_s}}, \quad (10)$$

$$r_{\text{exit}}^c \leq -U_{\text{out}} - \frac{1}{\gamma^{k_p - 1}} \left[ (U_{\text{in}} + r_{\text{in}}^c) \frac{1 + \gamma^{k_p - 1}(\gamma - 1)}{1 - \gamma} - \sigma \right]. \quad (11)$$

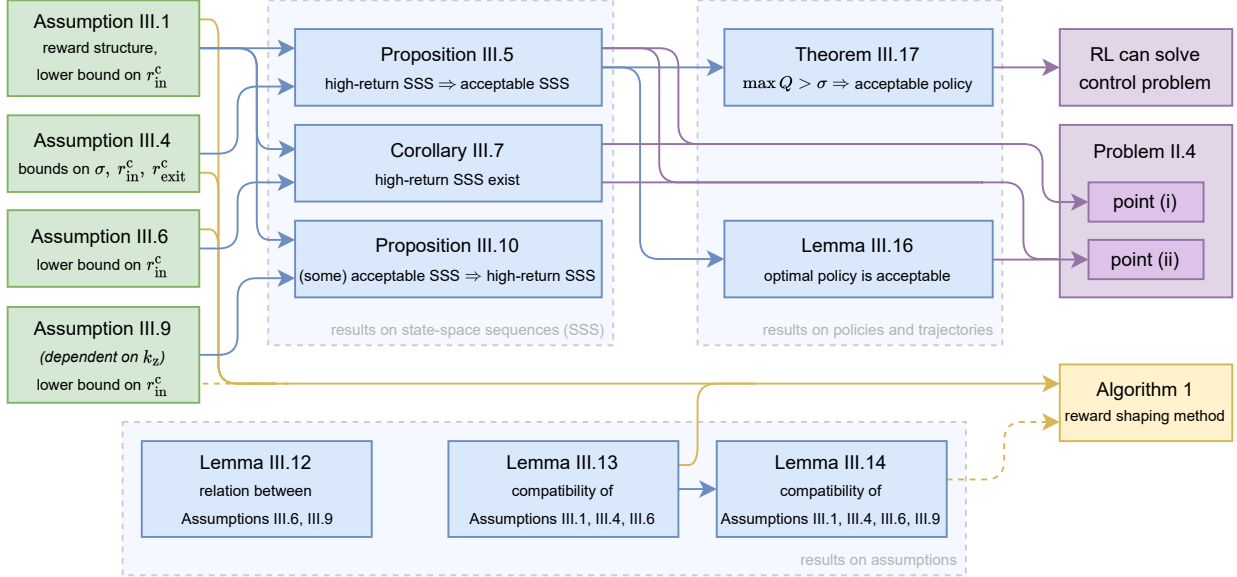


Fig. 2. Schematic representation of the main assumptions and results in Section III. Green blocks denote assumptions, blue blocks indicate analytical findings, yellow blocks denote algorithms, and purple blocks refer to the problems being studied. Dashed arrows denote optional steps in the control design. “SSS” means “state-space sequence”; The symbols in the figure are defined in Section III.

In the following Proposition, we state a key result that solves point (i) in Problem II.4.

**Proposition III.5.** *Let Assumptions III.1 and III.4 hold. Then, high-return state-space sequences are acceptable.*

*Proof.* We will show that, for any policy  $\pi$ , if a state-space sequence  $\xi$  is not acceptable, then it is not high-return (consequently, if  $\xi$  is high-return, then it is acceptable).

$\xi$  can be not acceptable if and only if one of the following three scenarios occurs (cf. Definition II.3):

- 1)  $\xi$  is never in the goal region  $\mathcal{G}$ ;
- 2)  $\xi$  is in  $\mathcal{G}$  for the first time at a time later than  $k_s$ ;
- 3)  $\xi$  exits from  $\mathcal{G}$  at time  $k_{\text{exit}}(\xi) \leq k_p$ .

We now consider the three cases one by one and show that, for any  $\pi$ , if any of them occurs then it must hold that  $\xi$  is not high-return, i.e.,  $J^\pi(\xi) \leq \sigma$ .

*Case 1:* In this case, the state-space sequence is never in the goal region, that is  $\forall k \in [0, \infty), x_k \notin \mathcal{G}$ . Therefore, only the third case in (6) is fulfilled, for all  $k$ , and we obtain  $r^c(x_k, x_{k-1}) = 0$  for all  $k$ . For any policy  $\pi$ , exploiting (2), (4), (5a), and (9), we obtain<sup>2</sup>

$$\begin{aligned} J^\pi(\xi) &= \sum_{k=1}^{+\infty} \gamma^{k-1} r^b(x_k, x_{k-1}, u_{k-1}) \\ &\leq U_{\text{out}} \sum_{k=1}^{+\infty} \gamma^{k-1} = \frac{U_{\text{out}}}{1-\gamma} \leq \sigma. \end{aligned} \quad (12)$$

Note that, in (12) and in the rest of the proof, the dependency of  $J^\pi$  on the specific policy  $\pi$  is made irrelevant by using the bounds in (5).

<sup>2</sup>Recall that, for  $|\gamma| < 1$ , the geometric series is  $\sum_{k=0}^{+\infty} \gamma^k = \frac{1}{1-\gamma}$  and the truncated geometric series is  $\sum_{k=0}^{n-1} \gamma^k = \frac{1-\gamma^n}{1-\gamma}$ .

*Case 2:* Defining  $k_{\text{enter}} := (\min k \text{ s.t. } x_k \in \mathcal{G})$ , we have that  $k_{\text{enter}} > k_s$ . For the sake of simplicity and without loss of generality, assume that the state is always in the region  $\mathcal{G}$  after  $k_{\text{enter}}$  (i.e.,  $x_k \in \mathcal{G}, \forall k \geq k_{\text{enter}}$ ).<sup>3</sup> For any policy  $\pi$ , from (2), (4), and (6), we obtain

$$\begin{aligned} J^\pi(\xi) &= \sum_{k=1}^{k_{\text{enter}}-1} \gamma^{k-1} r^b(x_k, x_{k-1}, u_{k-1}) \\ &\quad + \sum_{k=k_{\text{enter}}}^{+\infty} \gamma^{k-1} [r^b(x_k, x_{k-1}, u_{k-1}) + r_{\text{in}}^c]. \end{aligned} \quad (13)$$

Exploiting (7), and recalling that  $k_{\text{enter}} > k_s$ , from (13), we obtain

$$\begin{aligned} J^\pi(\xi) &\leq \sum_{k=1}^{k_s} \gamma^{k-1} r^b(x_k, x_{k-1}, u_{k-1}) \\ &\quad + \sum_{k=k_s+1}^{+\infty} \gamma^{k-1} [r^b(x_k, x_{k-1}, u_{k-1}) + r_{\text{in}}^c]. \end{aligned} \quad (14)$$

Then, from (14) and exploiting (5), we obtain

$$\begin{aligned} J^\pi(\xi) &\leq U_{\text{out}} \sum_{k=1}^{k_s} \gamma^{k-1} + (U_{\text{in}} + r_{\text{in}}^c) \sum_{k=k_s+1}^{+\infty} \gamma^{k-1} \\ &= U_{\text{out}} \sum_{k=0}^{k_s-1} \gamma^k + (U_{\text{in}} + r_{\text{in}}^c) \gamma^{k_s} \sum_{k=0}^{+\infty} \gamma^k \\ &= U_{\text{out}} \frac{1-\gamma^{k_s}}{1-\gamma} + (U_{\text{in}} + r_{\text{in}}^c) \frac{\gamma^{k_s}}{1-\gamma}. \end{aligned}$$

<sup>3</sup>The reason why we do not lose generality is that we are interested in upper bounding  $J^\pi(\xi)$  with  $\sigma$ , and the simplifying assumption makes  $J^\pi(\xi)$  the largest possible, because the smallest reward obtainable inside  $\mathcal{G}$  (i.e.,  $r_{\text{in}}^c + L_{\text{in}}$ ) is at least equal to the largest reward obtainable outside  $\mathcal{G}$  (i.e.,  $U_{\text{out}}$ ), because of (7).

Exploiting (10), it is immediate to see that  $J^\pi(\xi) \leq \sigma$ .

*Case 3:* From the definition of  $k_{\text{exit}}$  (see Sec. II), we have  $x_{k_{\text{exit}}(\xi)-1} \in \mathcal{G}$  and  $x_{k_{\text{exit}}(\xi)} \notin \mathcal{G}$ . From (7), the largest  $J^\pi(\xi)$  is obtained when the state-space sequence  $\xi$  is such that  $x_k \in \mathcal{G}, \forall k \in [1, k_{\text{exit}}(\xi))$ ,  $\xi$  then exits the region  $\mathcal{G}$  at  $k_{\text{exit}}(\xi) = k_p$ , and enters again at time  $k_p + 1$ . Thus, without loss of generality, we assume this is the case. Then, we have

$$\begin{aligned} J^\pi(\xi) &\leq \sum_{k=1}^{k_p-1} \gamma^{k-1} [r^b(x_k, x_{k-1}, u_{k-1}) + r_{\text{in}}^c] \\ &\quad + \gamma^{k_p-1} (r^b(x_{k_p}, x_{k_p-1}, u_{k_p-1}) + r_{\text{exit}}^c) \\ &\quad + \sum_{k=k_p+1}^{\infty} \gamma^{k-1} [r^b(x_k, x_{k-1}, u_{k-1}) + r_{\text{in}}^c] \\ &\leq (U_{\text{in}} + r_{\text{in}}^c) \left[ \sum_{k=0}^{k_p-2} \gamma^k + \gamma^{k_p} \sum_{k=0}^{\infty} \gamma^k \right] \\ &\quad + \gamma^{k_p-1} (U_{\text{out}} + r_{\text{exit}}^c) \\ &= (U_{\text{in}} + r_{\text{in}}^c) \frac{1 - \gamma^{k_p-1} + \gamma^{k_p}}{1 - \gamma} + \gamma^{k_p-1} (U_{\text{out}} + r_{\text{exit}}^c). \end{aligned}$$

Exploiting (11), we immediately verify that  $J^\pi(\xi) \leq \sigma$ .  $\square$

Notably, Proposition III.5 does not guarantee the existence of any high-return state-space sequence. The existence of the latter is instead guaranteed by Corollary III.7 below.

**Assumption III.6.** *Let*

$$r_{\text{in}}^c > \sigma(1 - \gamma) - L_{\text{in}}. \quad (15)$$

**Corollary III.7.** *Let Assumption III.1 hold. A sufficient condition for the existence of high-return state-space sequences is that Assumption III.6 holds. Moreover, a necessary condition for the existence of high-return state-space sequences is that*

$$r_{\text{in}}^c > \sigma(1 - \gamma) - U_{\text{in}}. \quad (16)$$

*Proof.* Let  $P$  be the proposition “ $\exists \xi \in \mathcal{X}^\infty : \forall \pi, J^\pi(\xi) > \sigma$ ”.

*Assumption III.6  $\Rightarrow P$ :* Consider a state-space sequence  $\xi^\diamond = (x_0, x_1, \dots)$  with all  $x_k \in \mathcal{G}$ . Then, for any  $\pi$ , from (2), (6) and (7), it holds that  $J^\pi(\xi^\diamond) \geq \frac{r_{\text{in}}^c + L_{\text{in}}}{1 - \gamma}$ . Exploiting Assumption III.6, we derive that  $J^\pi(\xi^\diamond) > \sigma$ .

*(16)  $\Leftarrow P$ :* To demonstrate this result, we show equivalently that  $\neg(16) \Rightarrow \neg P$ . Using again (2), (6) and (7), for any policy  $\pi$ , we derive that  $J^\pi(\xi) \leq \frac{r_{\text{in}}^c + U_{\text{in}}}{1 - \gamma}$  for all the state-space sequences  $\xi \in \mathcal{X}^\infty$ . If (16) does not hold, we have  $J^\pi(\xi) \leq \sigma, \forall \xi \in \mathcal{X}^\infty$ .  $\square$

We remark that although Assumption III.6 is not a necessary condition itself for the existence of high-return state-space sequences, it implies (16) (because of (8a)), which is one.

**Remark III.8** (Selection of  $k_p$ ). (11) captures the only assumption that depends on  $k_p$ . Given this assumption, it is possible to observe that  $k_p$  can be set to any arbitrarily large value, thus not limiting the variety of problems that can be addressed using the present theoretical framework.

To summarize, we demonstrated that it is possible to check if a state-space sequence is acceptable by verifying that it is

high-return. Conversely, there may exist acceptable state-space sequences that are not high-return, e.g., those that exit (and re-enter)  $\mathcal{G}$  before  $k_s$ , or those that enter  $\mathcal{G}$  before  $k_s$  but not early enough to collect sufficient rewards to be high-return. In some cases though, it is possible to prove that acceptable state-space sequences are high-return, such as those that enter the goal region not later than a certain time instant ( $k_z$ ) and never exit it, as formalized by the next Proposition.

**Assumption III.9** (Dependent on the choice of  $k_z$ ). *Given some  $k_z \in \mathbb{N}_{\geq 0}$ , with  $k_z \leq k_s$ , let*

$$r_{\text{in}}^c > -L_{\text{in}} - L_{\text{out}} \frac{1 - \gamma^{k_z-1}}{\gamma^{k_z-1}} + \sigma \frac{1 - \gamma}{\gamma^{k_z-1}}. \quad (17)$$

**Proposition III.10.** *Let  $k_z \in \mathbb{N}_{\geq 0}$  such that  $k_z \leq k_s$ . If Assumption III.1 and III.9 hold, then state-space sequences that are in  $\mathcal{G}$  for the first time at time  $k_z$  or earlier and have  $k_{\text{exit}} = \infty$  are high-return.*

*Proof.* According to the hypothesis, let  $\xi = (x_0, x_1, \dots)$  be a state-space sequence such that  $x_k \notin \mathcal{G}$  for  $k < k_z$  and  $x_k \in \mathcal{G}$  for  $k \geq k_z$ . For all policies  $\pi$ , from (2), (4) and (6), we obtain

$$\begin{aligned} J^\pi(\xi) &= \sum_{k=1}^{k_z-1} \gamma^{k-1} r^b(x_k, x_{k-1}, u_{k-1}) \\ &\quad + \sum_{k=k_z}^{+\infty} \gamma^{k-1} [r^b(x_k, x_{k-1}, u_{k-1}) + r_{\text{in}}^c]. \end{aligned}$$

Exploiting (5d) and (5c) yields

$$\begin{aligned} J^\pi(\xi) &\geq L_{\text{out}} \sum_{k=1}^{k_z-1} \gamma^{k-1} + (L_{\text{in}} + r_{\text{in}}^c) \sum_{k=k_z}^{+\infty} \gamma^{k-1} \\ &= L_{\text{out}} \sum_{k=0}^{k_z-2} \gamma^k + (L_{\text{in}} + r_{\text{in}}^c) \gamma^{k_z-1} \sum_{k=0}^{+\infty} \gamma^k \\ &= L_{\text{out}} \frac{1 - \gamma^{k_z-1}}{1 - \gamma} + (L_{\text{in}} + r_{\text{in}}^c) \frac{\gamma^{k_z-1}}{1 - \gamma}. \end{aligned}$$

Given (17), it follows that  $J^\pi(\xi) > \sigma$ . Moreover, say  $\xi'$  a state-space sequence that is in  $\mathcal{G}$  for the first time at some time  $k'_z < k_z$ , i.e., with  $x_k \notin \mathcal{G}$  for  $k < k'_z$  and  $x_k \in \mathcal{G}$  for  $k \geq k'_z$ . For all policies  $\pi$ , exploiting (7) and the fact that  $J^\pi(\xi) > \sigma$ , we have

$$\begin{aligned} J^\pi(\xi') &\geq L_{\text{out}} \sum_{k=1}^{k'_z-1} \gamma^{k-1} + (L_{\text{in}} + r_{\text{in}}^c) \sum_{k=k'_z}^{+\infty} \gamma^{k-1} \\ &\geq L_{\text{out}} \sum_{k=1}^{k_z-1} \gamma^{k-1} + (L_{\text{in}} + r_{\text{in}}^c) \sum_{k=k_z}^{+\infty} \gamma^{k-1} > \sigma. \end{aligned}$$

$\square$

From (17), we notice that the larger  $r_{\text{in}}^c$  is, the later state-space sequences are required to be in  $\mathcal{G}$  in order to be high-return. Moreover, it is again important to remark that while state-space sequences that enter  $\mathcal{G}$  within  $k_z$  time steps always exist, the same is not necessarily true for trajectories: this depends on the dynamics of the system being controlled.

**Remark III.11** (Tracking). *In the results in Section III-A, it was never assumed that  $\mathcal{G}$  is a fixed region in the state space. Indeed, it is possible to carry out the same analysis by considering a time-dependent goal region  $\mathcal{G}_k$  and, for simplicity of computation, the quantities*

$$U := \sup_{x' \in \mathcal{X}, x \in \mathcal{X}, u \in \mathcal{U}} r^b(x', x, u),$$

$$L := \inf_{x' \in \mathcal{X}, x \in \mathcal{X}, u \in \mathcal{U}} r^b(x', x, u)$$

rather than  $U_{\text{out}}$ ,  $U_{\text{in}}$ , and  $L_{\text{out}}$ ,  $L_{\text{in}}$  should be used in (5), respectively. This reformulation can be used to address tracking control problems.

Reviewing the findings derived so far, a shaped reward  $r$  needs to satisfy Assumptions III.1, III.4, III.6 (to exploits Proposition III.5 and Corollary III.7) and optionally Assumption III.9 (with some chosen  $k_z$ , to exploit Proposition III.10); see also Figure 2. Next, we characterize the relation between these assumptions and show that they can hold simultaneously.

### B. Compatibility of the assumptions

First, we give a Lemma to aid the selection of  $r_{\text{in}}^c$ .

**Lemma III.12.** *Given some  $k_z \leq k_s$ , if Assumption III.9 holds, Assumption III.6 also holds.*

*Proof.* See the Appendix.  $\square$

We say that two or more Assumptions are *compatible* if they can hold simultaneously. To guarantee that high-return state-space sequences are acceptable (Proposition III.5) and that such state-space sequences exist (Corollary III.7), we need Assumptions III.1, III.4, III.6, whose compatibility is ensured by the next Lemma.

**Lemma III.13.** *Assumptions III.1, III.4, III.6 are compatible if*

$$\sigma > \frac{U_{\text{out}}}{1-\gamma} + \frac{\Delta_{\text{in}} \gamma^{k_s}}{(1-\gamma)(1-\gamma^{k_s})}. \quad (18)$$

*Proof.* See the Appendix.  $\square$

To guarantee that a class of acceptable state-space sequences are high-return, we need Assumption III.9 (Proposition III.10), whose compatibility with previous ones is ensured by the next Lemma.

**Lemma III.14.** *Given some  $k_z \leq k_s$ , Assumptions III.1, III.4, III.6, III.9 are compatible if*

$$\sigma > \frac{\gamma^{k_s}}{(1-\gamma)(1-\gamma^{k_s})} \Delta_{\text{in}} + \frac{U_{\text{out}}}{1-\gamma} + \frac{\gamma^{k_s}(1-\gamma^{k_z-1})}{(1-\gamma)(\gamma^{k_z-1}-\gamma^{k_s})} \left( \frac{\gamma^{k_s} \Delta_{\text{in}}}{(1-\gamma^{k_s})} + \Delta_{\text{out}} \right). \quad (19)$$

*Proof.* See the Appendix.  $\square$

---

### Algorithm 1: Reward shaping

---

**Input:** A goal region  $\mathcal{G}$ , a desired settling time  $k_s$ , and a desired permanence time  $k_p$ ; a bounded reward function  $r^b$ , and discount factor  $\gamma$ .

**Output:** A reward function  $r$  satisfying to Assumptions III.1, III.4, III.6.

- 1  $U_{\text{out}} \leftarrow \sup_{x' \in \mathcal{X} \setminus \mathcal{G}, x \in \mathcal{X}, u \in \mathcal{U}} r^b(x', x, u);$   $\triangleright$  c.f. Eq. (5a)
  - 2  $U_{\text{in}} \leftarrow \sup_{x' \in \mathcal{G}, x \in \mathcal{X}, u \in \mathcal{U}} r^b(x', x, u);$   $\triangleright$  c.f. Eq. (5b)
  - 3  $L_{\text{in}} \leftarrow \inf_{x' \in \mathcal{G}, x \in \mathcal{X}, u \in \mathcal{U}} r^b(x', x, u);$   $\triangleright$  c.f. Eq. (5d)
  - 4  $\sigma \leftarrow \text{rand} \left( \frac{U_{\text{out}}}{1-\gamma} + \frac{(U_{\text{in}} - L_{\text{in}}) \gamma^{k_s}}{(1-\gamma)(1-\gamma^{k_s})}, \infty \right);$   $\triangleright$  from Lemma III.13
  - 5  $\mathcal{I} \leftarrow \left( \sigma(1-\gamma) - L_{\text{in}}, -U_{\text{in}} - U_{\text{out}} \frac{1-\gamma^{k_s}}{\gamma^{k_s}} + \sigma \frac{1-\gamma}{\gamma^{k_s}} \right);$   $\triangleright$  c.f. Eqs. (7), (10), (15)
  - 6  $r_{\text{in}}^c \leftarrow \text{rand}(\mathcal{I});$
  - 7  $r_{\text{exit}}^c \leftarrow \text{rand} \left( -\infty, \right.$   
 $\left. \rightarrow -U_{\text{out}} - \frac{1}{\gamma^{k_p-1}} \left[ (U_{\text{in}} + r_{\text{in}}^c) \frac{1+\gamma^{k_p-1}(\gamma-1)}{1-\gamma} - \sigma \right] \right);$   
 $\triangleright$  c.f. Eq. (11)
  - 8 build  $r^c$  as in (6);
  - 9  $r \leftarrow r^b + c;$
- 

### C. A constructive procedure for reward shaping

In Algorithm 1, we propose a constructive procedure that can be applied to shape the reward functions used in Section III. To provide more flexibility, the procedure takes a preexisting reward  $r^b$  as input, bounded according to (5). If no  $r^b$  is available, it is possible to set  $r^b = 0$ . As Lemma III.13 ensures set  $\mathcal{I}$  in the algorithm is not empty, the latter always terminates successfully. Once Algorithm 1 has been used to obtain a shaped reward  $r$  (thus fixing  $r_{\text{in}}^c$ ,  $r_{\text{exit}}^c$ ,  $\sigma$ , which remain constant), it is possible to run a reinforcement learning algorithm to learn a suitable control policy, as explained below in Section III-E.

It is to be noted that in some cases the values of  $r_{\text{in}}^c$  and  $r_{\text{exit}}^c$  resulting from Algorithm 1 might be significantly larger in absolute value when compared to those in  $r^b$ . This can lead to a relatively *sparse* reward function  $r$ , i.e., one where relatively large values (in absolute value) are present but infrequent in the state-action space. Notoriously, this lack of frequent feedback information can make learning more difficult, especially when deep reinforcement learning algorithms are used; see, e.g., [28], [29] and references therein. To mitigate this issue, it is possible to select  $r_{\text{in}}^c$  and  $r_{\text{exit}}^c$  as small in absolute value as possible, while still complying with Assumptions III.1, III.4, III.6. Reward shaping methods that do not make the reward sparse will be the subject of future work.

**Remark III.15** (Advanced reward shaping algorithm). *For simplicity, in Algorithm 1, we did not include the requirement captured by (17) on  $r_{\text{in}}^c$  (used to ensure that a family of acceptable state-space sequences are high-return, according to Proposition III.10), as it depends on the time instant  $k_z$ , which would be a further parameter to select. This constraint can be incorporated in Algorithm 1 by first selecting  $k_z \leq k_s$  (possibly exploiting knowledge of the system to control), enforcing (19) at line 4 (Lemma III.14 ensures  $\mathcal{I}$  is not empty), and using*

the right-hand side of (17) as lower bound of  $\mathcal{I}$  at line 5.

#### D. Assessing acceptable trajectories

In Section III-A, we showed how the value of the return  $J^\pi(\xi)$  can be used to assess whether  $\xi$  is an acceptable state-space sequence. The same theory applies to trajectories (which are state-space sequences, by definition).

It is important to remark that, while the existence of high-return state-space sequences is ensured by Proposition III.7, it can be much more difficult to establish if there actually exist policies that generate high-return trajectories. This depends on the dynamics of the system at hand and the performance required, and is tightly related to the problem of reachability [30], with the addition of requirements on the settling time and the permanence time.

#### E. Assessing acceptable policies in value-based reinforcement learning

First, we provide a simple result stating that an acceptable policy (see Definition II.3) can be found by achieving the optimum in (3), thus solving point (ii) in Problem II.4.

**Lemma III.16.** *Let Assumptions III.1 and III.4 hold. If there exists a high-return policy  $\pi^\diamond$  from  $\tilde{x}_0 \in \mathcal{X}$ , then the optimal policy  $\pi^*$  solving the problem objective defined in (3) is acceptable from  $\tilde{x}_0$ .*

*Proof.* As  $\pi^*$  maximizes the return in (3), then  $J^{\pi^*}(\phi^{\pi^*}(x_0)) \geq J^{\pi^\diamond}(\phi^{\pi^\diamond}(x_0)) > \sigma$ , exploiting Proposition III.5 (applicable, as Assumptions III.1 and III.4 hold).  $\square$

Proposition III.5 allows to detect acceptable state-space sequences by evaluating their return  $J^\pi$ . However, this is not normally known in a reinforcement learning setting, but it is instead approximated through a value function. In particular, let  $Q : \mathcal{X} \times \mathcal{U} \rightarrow \mathbb{R}$  be the state-action value function associated to the *greedy policy*

$$\pi_g(x) = \arg \max_{u \in \mathcal{U}} Q(x, u). \quad (20)$$

$Q$  is normally updated iteratively with the Bellman operator so that it converges to the value of  $J^{\pi_g}$ , in the sense that  $Q(x, u) \approx r(f(x, u), x, u) + \gamma J^{\pi_g}(\phi^{\pi_g}(f(x, u)))$  [31, Sec. 3].

In the next Theorem, we conclude the analysis by showing how the acceptability of a policy can be evaluated by assessing the value of  $Q$ .

**Theorem III.17.** *Consider a state  $x_k \in \mathcal{X}$  at time  $k$ . Let Assumptions III.1 and III.4 hold and assume that*

$$\text{sign} \left( \max_{u \in \mathcal{U}} Q(x_k, u) - \sigma \right) = \text{sign} (J^{\pi_g}(\phi^{\pi_g}(x_k)) - \sigma). \quad (21)$$

*If  $\max_{u \in \mathcal{U}} Q(x_k, u) > \sigma$ , then  $\pi_g$  is an acceptable policy from  $x_k$ .*

*Proof.* Exploiting (21),  $\max_{u \in \mathcal{U}} Q(x_k, u) > \sigma$  implies that  $J^{\pi_g}(\phi^{\pi_g}(x_k)) > \sigma$ . Thus, it is immediate to apply Proposition III.5 (using Assumptions III.1 and III.4) to obtain that  $\phi^{\pi_g}(x_k)$  is acceptable.  $\square$

It is important to clarify that  $\phi^{\pi_g}(x_k)$  being an acceptable trajectory means that, by following policy  $\pi_g$ , (i) the state-space sequence will be in  $\mathcal{G}$  before  $k_s$  time instants have passed (i.e.,  $\exists k' \in [k, k + k_s] : x_{k'} \in \mathcal{G}$ ), and (ii) the state will not exit from  $\mathcal{G}$  before  $k_p + 1$  time instants have passed, (i.e.,  $\nexists k'' \in [k + 1, k + k_p] : x_{k''-1} \in \mathcal{G}, x_{k''} \notin \mathcal{G}$ ). Moreover, we note that (21) is satisfied if  $Q$  is well approximating  $J^{\pi_g}$ , in the sense that

$$\left| \max_{u \in \mathcal{U}} Q(x_k, u) - J^{\pi_g}(\phi^{\pi_g}(x_k)) \right| < |J^{\pi_g}(\phi^{\pi_g}(x_k)) - \sigma|. \quad (22)$$

Indeed, (22) implies (21) through Lemma A.2 in the Appendix.<sup>4</sup> (22) is fulfilled after a finite number of iterations if the algorithm used to update the value of  $Q$  is converging asymptotically to  $J^{\pi_g}$ , which has been proved formally for reinforcement learning algorithms like SARSA and Q-learning [31]. In the latter, the greedy policy and the function  $Q$  are guaranteed to converge to the optimal policy and to its discounted return  $J$ , respectively; hence, if high-return policies exist, Lemma III.16 guarantees that the learned policy is acceptable.

## IV. NUMERICAL RESULTS

We validate the theory presented in Section III by means of two representative case studies (and corresponding reinforcement learning environments, from OpenAI Gym [22]): Inverted Pendulum [23] and Lunar Lander [24]. The former is a classic nonlinear benchmark problem in control theory, whereas the latter is a more sophisticated control problem with multiple input and outputs. In particular, we first validate Theorem III.17 using Q-learning to learn a policy that stabilizes an inverted pendulum within a predefined time; then, we show that the theory also holds when using a deep reinforcement learning algorithm, such as Double DQN, to learn a policy able to land a spacecraft fulfilling desired time constraints.

In each scenario, the learning phase and deployment phase are repeated in  $S \in \mathbb{N}_{>0}$  independent sessions, which are composed of  $E \in \mathbb{N}_{>0}$  episodes. Each episode is a simulation lasting  $N \in \mathbb{N}_{>0}$  time steps. Moreover, we always use the  $\epsilon$ -greedy policy [31] during learning.

For reproducibility, the code is available on GitHub [25].

### A. Inverted Pendulum

1) *Description of the Inverted Pendulum environment:* In this environment, the objective is to stabilize a rigid pendulum affected by gravity to the upward position in a certain time, by exploiting a torque applied at the joint. In particular, the pendulum is a rigid rod, having length  $l = 1$  m, mass  $m = 1$  kg and moment of inertia  $I = ml^2/3$ ; the gravitational acceleration is taken equal to  $g = 10$  m/s<sup>2</sup>. A graphical depiction of the scenario is given in Figure 3a.

<sup>4</sup>Assuming  $J^{\pi_g}(\phi^{\pi_g}(x_k)) \neq \sigma$ . The case that  $J^{\pi_g}(\phi^{\pi_g}(x_k)) = \sigma$  is however not of interest, as the trajectory  $\phi^{\pi_g}(x_k)$  would not be high-return.



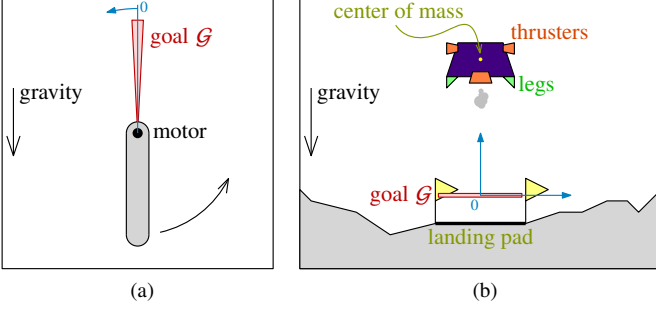


Fig. 3. Sketch representation of the environments used in the numerical validation in Section IV: (a) Inverted Pendulum and (b) Lunar Lander. Both the pendulum and the lander are depicted in their initial states.

a) *State*: The state at time  $k$  is  $x_k := [x_{k,1} \ x_{k,2}]^T$ , where  $x_{k,1}$  and  $x_{k,2}$  are the angular position and angular velocity of the pendulum, respectively. In order to apply Q-learning, which is a tabular RL method, we discretize the state space (and the set of acceptable inputs). Namely, the position  $x_{k,1}$  takes values in  $[-\pi, \pi]$  rad, with  $[-\pi, -\frac{\pi}{9}]$  discretized into 8 equally spaced values,  $(-\frac{\pi}{9}, -\frac{\pi}{36}]$  into 7 values, and  $(-\frac{\pi}{36}, 0]$  into 5 values (analogously for  $[0, \pi]$ ). The velocity  $x_{k,2}$  takes values in  $[-8, 8]$  rad/s, with  $[-8, -1]$  discretized into 10 values, and  $(-1, 0]$  into 9 values (analogously for  $[0, 8]$ ).  $x_{k,1} = 0$  and  $x_{k,1} = \pi$  correspond to the upward and downward positions, respectively. In each simulation the initial condition is chosen as  $x_0 = [\pi \ 0]^T$ .

b) *Control inputs*: The control input  $u_k$  is a torque applied at the pendulum's rotating joint, with values chosen in  $[-2, 2]$  Nm, with the interval  $[-2, -0.2]$  discretized into 9 values, and  $(-0.2, 0]$  into 4 values (analogously for  $[0, 2]$ ).

c) *Control problem*: Let  $x^{\text{ref}} := [0 \ 0]^T$  denote the unstable vertical position. The goal region is  $\mathcal{G} := \{x \in \mathcal{X} \mid \|x - x^{\text{ref}}\| < \theta\}$  ( $\|\cdot\|$  being the Euclidean norm), with  $\theta = 0.42$  amounting to 5% of the maximum distance from the origin, in the state space. We select the desired settling time as  $k_s = 500$  time steps and the desired permanence time as  $k_p = 1000$  time steps (cf. Sec. II).

d) *Reward*: To guarantee the required performance and steady-state specifications, the reward function is chosen as in (4), with  $r^b$  being the standard Gym reward, given by

$$r^b(x_k, x_{k-1}, u_{k-1}) = -x_{1,k}^2 - 0.1x_{2,k}^2 - 0.001u_{k-1}^2. \quad (23)$$

Following Algorithm 1, from (23), we compute that

$$U_{\text{out}} = \max_{x_k \notin \mathcal{G}, x_{k-1} \in \mathcal{X}, u_{k-1} \in \mathcal{U}} r^b = -0.1\theta^2 \approx -0.018,$$

$$L_{\text{out}} = \min_{x_k \notin \mathcal{G}, x_{k-1} \in \mathcal{X}, u_{k-1} \in \mathcal{U}} r^b \\ = -\pi^2 - 0.1 \cdot 8^2 - 0.001 \cdot 2^2 \approx -16.27,$$

$$U_{\text{in}} = \max_{x_k \in \mathcal{G}, x_{k-1} \in \mathcal{X}, u_{k-1} \in \mathcal{U}} r^b = 0,$$

$$L_{\text{in}} = \min_{x_k \in \mathcal{G}, x_{k-1} \in \mathcal{X}, u_{k-1} \in \mathcal{U}} r^b = -\theta^2 - 0.001 \cdot 2^2 \approx -0.18.$$

Then, given  $\gamma = 0.99$  [cf. (2)], we select  $\sigma = 10000$  [cf. (9)], and the correction terms in (6) as

$$r_{\text{in}}^c = -U_{\text{in}} - U_{\text{out}} \frac{1 - \gamma^{k_s}}{\gamma^{k_s}} + \sigma \frac{1 - \gamma}{\gamma^{k_s}} \approx 1.52 \cdot 10^4,$$

$$r_{\text{exit}}^c = -U_{\text{out}} - \frac{1}{\gamma^{k_p-1}} \left[ (U_{\text{in}} + r_{\text{in}}^c) \frac{1 + \gamma^{k_p-1}(\gamma - 1)}{1 - \gamma} - \sigma \right] \\ \approx -3.50 \cdot 10^{10}.$$

e) *Parameters*: We take  $S = 5$  sessions,  $E = 1000$  episodes, and  $N = 1000$  time steps. We set the learning rate to 0.8. For the  $\epsilon$ -greedy policy, we select  $\epsilon = 0.05$ .

2) *Results of Q-learning in the Inverted Pendulum environment*: After training is completed for all sessions, we test the capability of the learned policies to swing up and stabilize the pendulum within the desired settling time. The results are portrayed in Figure 4, showing the distance of the trajectories from  $x^{\text{ref}}$ , position, and velocity in time. We observe that the control problem is solved in all sessions, suggesting that the optimal policy (which would be an acceptable one, according to Lemma III.16) has been found. Interestingly, this might be difficult to detect by looking only at the returns obtained during training, plotted in Figure 5. Indeed, the discounted returns per episode appear to decrease as training progresses. This happens because, as the agent progressively learns to enter the goal region, and to do so earlier in later episodes, the chance of it incurring the penalty  $r_{\text{exit}}^c$  for existing the goal region increases as the result of random explorative actions, taken by the  $\epsilon$ -greedy policy used during learning. Although this does not prevent learning from converging to the optimal policy, in practical implementations, this can be avoided by letting the exploration rate  $\epsilon$  decay in later episodes. However, tuning the decay rate is highly problem-dependent and no general rule can therefore be given here.

In our experiments, learning ended after the planned episodes. An alternative heuristic method to determine when to terminate the learning stage is to pause training at regular intervals, and simulate using the greedy policy in (20). If the return obtained exceeds  $\sigma$ , the greedy policy is deemed acceptable (see Proposition III.5), ending learning; otherwise, training continues.

## B. Lunar Lander

1) *Description of the Lunar Lander environment*: In a 2D space, a stylized spaceship must land with small speed in a specific area in a predetermined time, in the presence of gravity, and in the absence of friction. The spacecraft has three thrusters to guide its descent and two supporting legs at the bottom, as depicted in Figure 3b.

a) *State*: The state at time  $k$  is  $x_k = [p_k^T \ v_k^T \ \theta_k \ \omega_k \ l_k^l \ l_k^r]^T$ , where  $p_k \in \mathbb{R}^2$  is the horizontal and vertical position of the center of mass (arbitrary units; a.u.),  $v_k \in \mathbb{R}^2$  is its horizontal and vertical velocity (a.u./s),  $\theta_k \in [0, 2\pi]$  rad is the orientation of the lander (with 0 corresponding to the orientation of a correctly landed spacecraft),  $\omega_k$  is the rate of change of the orientation (rad/s),  $l_k^l \in \{0, 1\}$  (resp.  $l_k^r$ ) is 1 if the left (resp. right) leg is touching the ground. The initial conditions are given by  $p_0 = [0 \ 1.4]^T$  (consequently,  $l_0^l = l_0^r = 0$ ),  $v_0 = [0 \ 0]^T$ ,  $\theta_0 = 0$ , and  $\omega_0 = 0$ . The landing area is the region  $[-0.2 \ 0.2] \times [-0.001 \ 0.001]$  (horizontal and vertical intervals, respectively). The terrain topography (beyond the landing pad) is random in each simulation.



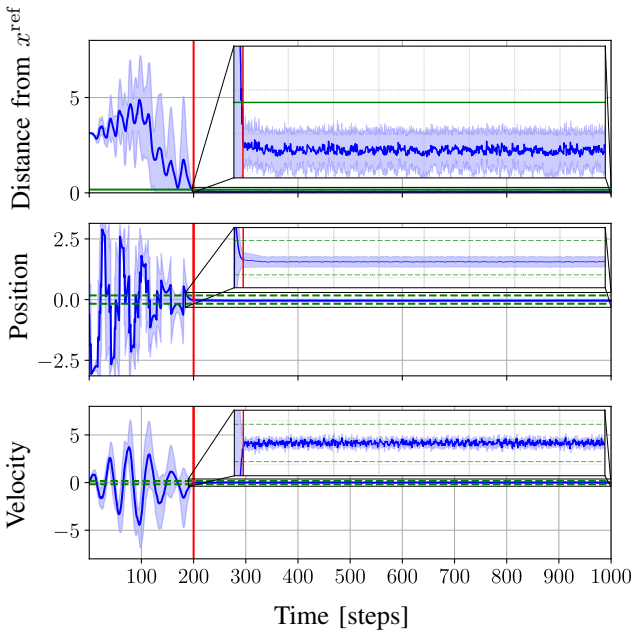


Fig. 4. Average (blue line) plus/minus standard deviation (shaded area) of  $\|x_k - x^{\text{ref}}\|$  (top panel), angular position  $x_{k,1}$  (middle panel), and angular velocity  $x_{k,2}$  (bottom panel), obtained by  $S$  policies trained with Q-learning in the pendulum environment. The green solid line (top panel) indicates the goal region  $\mathcal{G}$ ; the green dashed line (middle and bottom panel) indicate neighborhoods of width  $2\theta$  centered in  $x_{1,k} = x_1^{\text{ref}} = 0$  (middle panel) and in  $x_{2,k} = x_2^{\text{ref}} = 0$  (bottom panel). The red line indicates the time instant when the (averaged) trajectory enters the goal region.

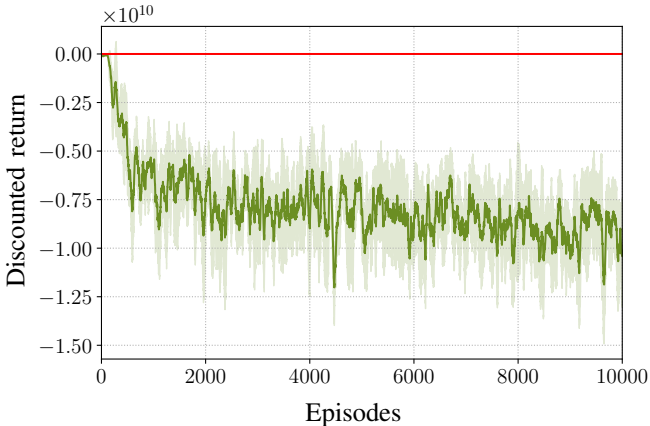


Fig. 5. Average (green line) plus/minus standard deviation (shaded area) of the discounted returns per episode obtained in  $S$  training sessions with Q-learning in the pendulum environment. The red line indicates the threshold value  $\sigma$  (cf. Sec. III-A). The returns are averaged backwards across episodes using a moving window of 50 samples.

*b) Control inputs:* At each time step  $k$ , the lander can use at most one of its three thrusters. In particular, we let  $u_k^m \in \{0, 1\}$  be 1 if at time  $k$  the main engine on the bottom of the spacecraft is used at full power or 0 if it is off, and define  $u_k^l, u_k^r \in \{0, 1\}$  analogously for the left and right thrusters, respectively. Then, the control input at time  $k$  is the vector  $u_k = [u_k^m \ u_k^l \ u_k^r]^T$ , which has four possible values, depending on which thruster, if any, is used.

*c) Control problem:* The goal region  $\mathcal{G}$  is the set of states where  $p_k$  is in the landing pad,  $v_k = 0$ ,  $\theta_k = \omega_k = 0$ , and

$l_k^l = l_k^r = 1$ . Additionally, we select the desired settling time as  $k_s = 500$  time steps and the desired permanence time as  $k_p = 1000$  time steps (cf. Section II). We also remark that the simulation stops if the lander touches the ground beyond the landing pad, or if it lands on the pad with a speed that is too high. During training only, the simulation is also halted if the spacecraft lands correctly. Further detail can be found in [24].

*d) Reward:* The reward function is in the form introduced in (4), with  $r^b$  generated according to the standard environment definition [24]. Namely, let  $\hat{r}: \mathcal{X} \times \mathcal{X} \times \mathcal{U} \rightarrow \mathbb{R}$  be a function given by

$$\begin{aligned} \hat{r}(x_k, x_{k-1}, u_{k-1}) := & 100(\|p_k\| - \|p_{k-1}\|) \\ & + 100(\|v_k\| - \|v_{k-1}\|) + 100(|\theta_k| - |\theta_{k-1}|) \\ & + 10(l_k^l - l_{k-1}^l) + 10(l_k^r - l_{k-1}^r) \\ & + 0.3u_{k-1}^m + 0.03u_{k-1}^l + 0.03u_{k-1}^r. \end{aligned} \quad (24)$$

Then,  $r^b$  is given by

$$r^b(x_k, x_{k-1}, u_{k-1}) = \begin{cases} 100 & \text{if } \beta_1 \text{ is true,} \\ -100 & \text{if } \beta_2 \text{ is true,} \\ \hat{r} & \text{otherwise,} \end{cases} \quad (25)$$

where  $\beta_1$  and  $\beta_2$  are two mutually exclusive Boolean conditions: namely,  $\beta_1$  is true if the spacecraft lands on the ground and stops, and  $\beta_2$  becomes true if the lander touches any point of the map with a speed that is too high (i.e., it crashes), or goes beyond the operating area of the environment, i.e.,  $[-1.5, 1.5] \times [-1.5, 1.5]$ . Following Algorithm 1, from (25), we derive that  $U_{\text{out}} = 100$ ,  $L_{\text{out}} = -100$ ,  $U_{\text{in}} = 100$ ,  $L_{\text{in}} = 100$ . Given  $\gamma = 0.99$  (cf. (2)), we select  $\sigma = 12000$  (cf. (9)), and the correction terms in (6) as

$$\begin{aligned} r_{\text{in}}^c &= -U_{\text{in}} - U_{\text{out}} \frac{1 - \gamma^{k_s}}{\gamma^{k_s}} + \sigma \frac{1 - \gamma}{\gamma^{k_s}} \approx 3.04 \cdot 10^3, \\ r_{\text{exit}}^c &= -U_{\text{out}} - \frac{1}{\gamma^{k_p - 1}} \left[ (U_{\text{in}} + r_{\text{in}}^c) \frac{1 + \gamma^{k_p - 1}(\gamma - 1)}{1 - \gamma} - \sigma \right] \\ &\approx -6.93 \cdot 10^9. \end{aligned}$$

*e) Parameters:* We take  $S = 5$  sessions,  $E = 1000$  episodes, and  $N = 1000$  time steps. For the  $\epsilon$ -greedy policy, we select  $\epsilon = 0.1$ . To better stabilize the values of  $Q$  and help prevent overestimation, we use a standard *Double DQN* algorithm (a variation of *DQN* [32]; see [33] for a detailed description), implemented in TensorFlow 2. For the neural networks, we used an input layer with 8 nodes, 2 hidden layers each composed of 128 nodes with rectified linear unit (ReLU) activation functions, and an output layer with 3 nodes and linear activation functions. The networks were trained using the Adam optimizer [34], with a learning rate of 0.001. Samples collected during training are stored in a replay buffer and at each training update a batch of 128 samples is used.

*2) Results of Double DQN in the Lunar Lander environment:* In this environment, in all sessions, the policies learned with Double DQN are able to solve the given control problem, fulfilling the given control requirements, as showed in Figure 6. In Figure 7, we also report the returns obtained by the learning algorithm. It is possible to observe that we obtain (averaged) returns that are over the threshold value  $\sigma$ . In this

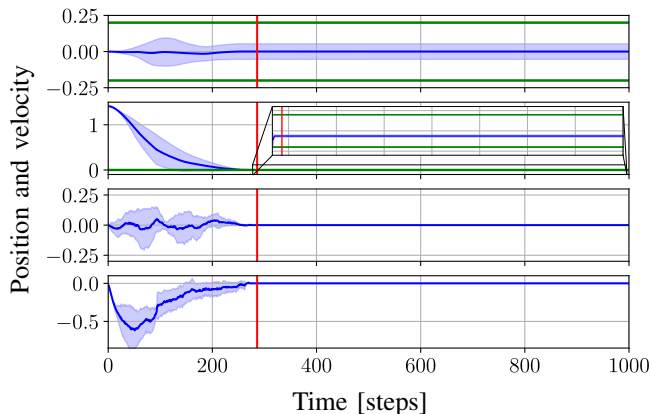


Fig. 6. Average (blue line) plus/minus standard deviation (shaded area) of the trajectory obtained by  $S$  policies trained with Double DQN in the Lunar Lander environment. From top to bottom: position on horizontal axis, position on vertical axis, velocity on horizontal axis, velocity on vertical axis. The green lines define the goal region. The red line indicates when the (averaged) trajectory enters the goal region.

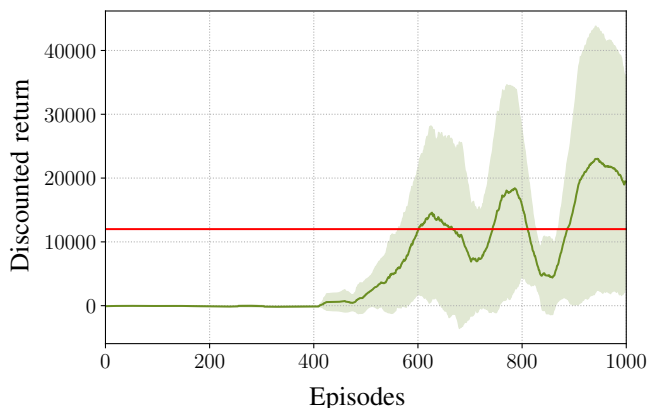


Fig. 7. Average (green line) plus/minus standard deviation (shaded area) of the discounted returns per episode obtained in  $S$  training sessions with Double DQN in the Lunar Lander environment. The red line indicates the threshold value  $\sigma$  (cf. Sec. III-A). The returns are averaged backwards across episodes using a moving window of 50 samples.

case, the large negative returns, which were visible in Figure 5 for the Inverted Pendulum environment, are not present. The reason is that, in the Lunar Lander simulation environment, during training (but not on validation), once the lander stops, the simulation is halted; therefore, in this case, during training the lander never exits the goal region once it has entered it.

## V. CONCLUSIONS

One of the most significant issues holding back the use of reinforcement learning for control applications is the lack of guarantees concerning the performance of the learned policies. In this work, we have presented analytical results that show how a specific shaping of the reward function can ensure that a control problem, such as a regulation problem, is solved with arbitrary precision, within a given settling time. We have validated the proposed theoretical approach on two representative experimental scenarios: the stabilization of an inverted pendulum and the landing of a simplified spacecraft.

One drawback of the present methodology is that the shaped reward might be relatively sparse (as discussed in Section III-C), which could possibly hamper learning when using deep reinforcement learning algorithms. Future work will focus on integrating existing techniques [35] (and developing new ones) for reward shaping, which are able to deal with the potential sparse reward problem, on extending the current results to the case of stochastic system dynamics, and on deriving conditions to ensure feasibility of a set of control requirements ( $\mathcal{G}$ ,  $k_s$ ,  $k_p$ ) for a given system, which is highly problem-dependent.

## REFERENCES

- [1] H. Dong, X. Zhao, and H. Yang, "Reinforcement learning-based approximate optimal control for attitude reorientation under state constraints," *IEEE Transactions on Control Systems Technology*, vol. 29, no. 4, pp. 1664–1673, 2021.
- [2] H. Dong and X. Zhao, "Data-driven wind farm control via multiplayer deep reinforcement learning," *IEEE Transactions on Control Systems Technology*, vol. 31, no. 3, pp. 1468–1475, 2023.
- [3] B. R. Kiran, I. Sobh, V. Talpaert, P. Mannion, A. A. A. Sallab, S. Yogamani, and P. Pérez, "Deep reinforcement learning for autonomous driving: A survey," *IEEE Transactions on Intelligent Transportation Systems*, vol. 23, no. 6, pp. 4909–4926, 2022.
- [4] J. Degraeve, F. Felici, J. Buchli, M. Neunert, B. Tracey, F. Carpanese, T. Ewalds, R. Hafner, A. Abdolmaleki, D. de Las Casas *et al.*, "Magnetic control of tokamak plasmas through deep reinforcement learning," *Nature*, vol. 602, no. 7897, pp. 414–419, 2022.
- [5] F. L. Lewis and D. Vrabie, "Reinforcement learning and adaptive dynamic programming for feedback control," *IEEE Circuits and Systems Magazine*, vol. 9, no. 3, pp. 32–50, 2009.
- [6] P. Osinenko, D. Dobriborsci, and W. Aumer, "Reinforcement learning with guarantees: A review," *IFAC-PapersOnLine*, vol. 55, no. 15, pp. 123–128, 2022.
- [7] J. Randløv and P. Alstrøm, "Learning to drive a bicycle using reinforcement learning and shaping," in *Proceedings of the 15th International Conference on Machine Learning (ICML 1998)*, 1998, pp. 463–471.
- [8] A. Y. Ng, D. Harada, and S. Russell, "Policy invariance under reward transformations: Theory and application to reward shaping," in *Proceedings of the 16th International Conference on Machine Learning (ICML 1999)*, 1999, pp. 278–287.
- [9] A. Gupta, A. Pacchiano, Y. Zhai, S. Kakade, and S. Levine, "Unpacking reward shaping: Understanding the benefits of reward engineering on sample complexity," in *Advances in Neural Information Processing Systems (NeurIPS 2022)*, vol. 35, 2022, pp. 15 281–15 295.
- [10] Y. Dong, X. Tang, and Y. Yuan, "Principled reward shaping for reinforcement learning via lyapunov stability theory," *Neurocomputing*, vol. 393, pp. 83–90, 2020.
- [11] T. J. Perkins and A. G. Barto, "Lyapunov design for safe reinforcement learning," *Journal of Machine Learning Research*, vol. 3, no. 4/5, pp. 803–832, 2002.
- [12] F. Berkenkamp, M. Turchetta, A. Schoellig, and A. Krause, "Safe model-based reinforcement learning with stability guarantees," in *Advances in Neural Information Processing Systems (NeurIPS 2017)*, 2017.
- [13] Y. Chow, O. Nachum, E. Duenez-Guzman, and M. Ghavamzadeh, "A Lyapunov-based approach to safe reinforcement learning," in *Advances in Neural Information Processing Systems (NeurIPS 2018)*, 2018, pp. 1–10.
- [14] M. Alshiekh, R. Bloem, R. Ehlers, B. Könighofer, S. Niekum, and U. Topcu, "Safe reinforcement learning via shielding," *Proceedings of the 32nd AAAI Conference on Artificial Intelligence (AAAI 2018)*, vol. 32, no. 1, 2018.
- [15] Z. Marvi and B. Kiumarsi, "Safe reinforcement learning: A control barrier function optimization approach," *International Journal of Robust and Nonlinear Control*, vol. 31, no. 6, pp. 1923–1940, 2021.
- [16] L. Beckenbach, P. Osinenko, and S. Streif, "A Q-learning predictive control scheme with guaranteed stability," *European Journal of Control*, vol. 56, pp. 167–178, 2020.
- [17] R. E. Kalman, "When is a linear control system optimal?" *Journal of Basic Engineering*, vol. 86, no. 1, pp. 51–60, 03 1964.
- [18] A. E. Bryson, "Optimal control—1950 to 1985," *IEEE Control Systems Magazine*, vol. 16, pp. 26–33, 1996.

- [19] L. Rodrigues, “Inverse optimal control with discount factor for continuous and discrete-time control-affine systems and reinforcement learning,” in *2022 61st IEEE Conference on Decision and Control (CDC 2022)*, 2022, pp. 5783–5788.
- [20] E. Garrabé, H. Jesawada, C. Del Vecchio, and G. Russo, “On a probabilistic approach for inverse data-driven optimal control,” in *2023 62nd IEEE Conference on Decision and Control (CDC)*, 2023, pp. 4411–4416.
- [21] T. Jouini and A. Rantzer, “On cost design in applications of optimal control,” *IEEE Control Systems Letters*, vol. 6, pp. 452–457, 2022.
- [22] G. Brockman, V. Cheung, L. Pettersson, J. Schneider, J. Schulman, J. Tang, and W. Zaremba, “OpenAI Gym,” *arXiv preprint arXiv:1606.01540*, 2016.
- [23] OpenAI, *OpenAI Gym Inverted Pendulum Online Documentation*, 2022. [Online]. Available: [https://www.gymnasium.dev/environments/classic\\_control/pendulum/](https://www.gymnasium.dev/environments/classic_control/pendulum/)
- [24] —, *OpenAI Gym Lunar Lander Online Documentation*, 2022. [Online]. Available: [https://www.gymnasium.dev/environments/box2d/lunar\\_lander/](https://www.gymnasium.dev/environments/box2d/lunar_lander/)
- [25] F. De Lellis, *Reward shaping for RL based control*, 2023. [Online]. Available: <https://github.com/FrancescoDeLellis/Reward-shaping-for-RL-based-control>
- [26] F. De Lellis, M. Coraggio, G. Russo, M. Musolesi, and M. di Bernardo, “CT-DQN: Control-tutored deep reinforcement learning,” in *Proceedings of the 5th Annual Learning for Dynamics and Control Conference (LADC 2023)*, ser. Proceedings of Machine Learning Research, vol. 211, 2023, pp. 941–953.
- [27] F. De Lellis, M. Coraggio, G. Russo, M. Musolesi, and M. di Bernardo, “Control-tutored reinforcement learning: Towards the integration of data-driven and model-based control,” in *Proceedings of the 4th Annual Learning for Dynamics and Control Conference (LADC 2022)*, ser. Proceedings of Machine Learning Research, vol. 168, 2022, pp. 1048–1059.
- [28] M. Riedmiller, R. Hafner, T. Lampe, M. Neunert, J. Degraeve, T. Wiele, V. Mnih, N. Heess, and J. T. Springenberg, “Learning by playing solving sparse reward tasks from scratch,” in *Proceedings of the 35th International Conference on Machine Learning (ICML 2018)*, ser. Proceedings of Machine Learning Research, vol. 80, 2018, pp. 4344–4353.
- [29] D. Rengarajan, G. Vaidya, A. Sarvesh, D. Kalathil, and S. Shakkottai, “Reinforcement learning with sparse rewards using guidance from offline demonstration,” in *International Conference on Learning Representations (ICLR 2022)*, 2022, pp. 1–21.
- [30] K. J. Åström and R. M. Murray, *Feedback Systems: An Introduction for Scientists and Engineers*, 2nd ed. Princeton University Press, 2021.
- [31] R. S. Sutton and A. G. Barto, *Reinforcement Learning: An Introduction*. The MIT Press, 2018.
- [32] V. Mnih, K. Kavukcuoglu, D. Silver, A. A. Rusu, J. Veness, M. G. Bellemare, A. Graves, M. Riedmiller, A. K. Fidjeland, G. Ostrovski et al., “Human-level control through deep reinforcement learning,” *Nature*, vol. 518, no. 7540, p. 529, 2015.
- [33] H. van Hasselt, A. Guez, and D. Silver, “Deep reinforcement learning with double Q-learning,” in *Proceedings of the 30th AAAI Conference on Artificial Intelligence (AAAI 2016)*. AAAI Press, 2016, pp. 2094–2100.
- [34] D. P. Kingma and J. Ba, “Adam: A method for stochastic optimization,” *arXiv preprint arXiv:1412.6980*, 2014.
- [35] F. Memarian, W. Goo, R. Lioutikov, S. Niekum, and U. Topcu, “Self-supervised online reward shaping in sparse-reward environments,” in *Proceedings of the 2021 IEEE/RSJ International Conference on Intelligent Robots and Systems (IROS 2021)*. IEEE, 2021, pp. 2369–2375.

## APPENDIX

Let  $\delta_{\mathcal{G}}(x) := \min_{y \in \mathcal{G}} \|x - y\|$  be the distance between  $x$  and  $\mathcal{G}$ ; let  $h(x, u) := f(x, u) - x$ , and let  $H := \sup_{x \in \mathcal{X}, u \in \mathcal{U}} \|g(x, u)\|$ .

**Proposition A.1.** *Consider the system defined in (1), and let  $H$  be finite. If  $k_s < \delta_{\mathcal{G}}(\tilde{x}_0)/H$ , there does not exist an acceptable policy  $\pi$  from  $\tilde{x}_0$ .*

*Proof.* We will show that there does not exist a policy  $\pi$  such that in  $\phi^\pi(\tilde{x}_0)$  there exist some  $k' \leq k_s$  such that  $x_{k'} \in \mathcal{G}$ .

Namely, consider some policy  $\pi$  and the trajectory  $\phi^\pi(\tilde{x}_0)$ ; note that

$$\begin{aligned} \delta_{\mathcal{G}}(\tilde{x}_0) &= \min_{y \in \mathcal{G}} \|\tilde{x}_0 - y\| = \min_{y \in \mathcal{G}} \|\tilde{x}_0 - x_k + x_k - y\| \\ &\leq \min_{y \in \mathcal{G}} (\|\tilde{x}_0 - x_k\| + \|x_k - y\|) \\ &= \|\tilde{x}_0 - x_k\| + \min_{y \in \mathcal{G}} \|x_k - y\|. \end{aligned} \quad (26)$$

Rewrite (26) as

$$\min_{y \in \mathcal{G}} \|x_k - y\| = \delta_{\mathcal{G}}(x_k) \geq \delta_{\mathcal{G}}(\tilde{x}_0) - \|\tilde{x}_0 - x_k\|. \quad (27)$$

A necessary condition for obtaining  $x_k \in \mathcal{G}$  is that  $\delta_{\mathcal{G}}(x_k) = 0$ , which is possible only if

$$\|\tilde{x}_0 - x_k\| \geq \delta_{\mathcal{G}}(\tilde{x}_0). \quad (28)$$

At the same time, it holds that

$$\|\tilde{x}_0 - x_k\| = \left\| \tilde{x}_0 - \left( \tilde{x}_0 + \sum_{j=0}^{k-1} g(x_j, u_j) \right) \right\| \leq kH. \quad (29)$$

Thus, to satisfy (28), it is required that  $kH \geq \delta_{\mathcal{G}}(\tilde{x}_0)$ . Hence, if  $k_s < \delta_{\mathcal{G}}(\tilde{x}_0)/H$ , then surely  $x_k \notin \mathcal{G}$  for all  $k \leq k_s$ , and thus  $\phi^\pi(\tilde{x}_0)$  is not acceptable.  $\square$

*Proof of Lemma III.12.* We rewrite (17) as

$$r_{\text{in}}^c > -L_{\text{in}} + \frac{1 - \gamma^{k_z - 1}}{\gamma^{k_z - 1}} [(1 - \gamma)\sigma - L_{\text{out}}] + (1 - \gamma)\sigma. \quad (30)$$

Exploiting (9) and (8b), we have  $(1 - \gamma)\sigma \geq U_{\text{out}} \geq L_{\text{out}}$ , that is  $(1 - \gamma)\sigma - L_{\text{out}} \geq 0$ . Thus, (30) implies (15).  $\square$

*Proof of Lemma III.13.* Assumptions III.1, III.4, III.6 are compatible if it is possible to select the constants  $\sigma$ ,  $r_{\text{in}}^c$ ,  $r_{\text{exit}}^c$  in accordance with (9), (7), (10), (11), (15). It is always possible to select some  $r_{\text{exit}}^c$  that satisfies to (11); differently, to have (9), (7), (10), (15) be compatible, the following must hold:

- (a) (9),
- (b)  $U_{\text{out}} - L_{\text{in}} \leq -U_{\text{in}} - U_{\text{out}} \frac{1 - \gamma^{k_s}}{\gamma^{k_s}} + \sigma \frac{1 - \gamma}{\gamma^{k_s}}$  [from (7) and (10)].
- (c)  $\sigma(1 - \gamma) - L_{\text{in}} < -U_{\text{in}} - U_{\text{out}} \frac{1 - \gamma^{k_s}}{\gamma^{k_s}} + \sigma \frac{1 - \gamma}{\gamma^{k_s}}$  [from (10) and (15)].

Note that (a) holds if  $\sigma \geq \frac{U_{\text{out}}}{1 - \gamma}$ , (b) holds if  $\sigma \geq \frac{U_{\text{out}}}{1 - \gamma} + \frac{\Delta_{\text{in}} \gamma^{k_s}}{1 - \gamma}$ , and (c) holds if (18) holds, which is the most restrictive of the three.  $\square$

*Proof of Lemma III.14.* From (10) and (17), Assumptions III.9 and III.4 are compatible if

$$\begin{aligned} -L_{\text{in}} - L_{\text{out}} \frac{1 - \gamma^{k_z - 1}}{\gamma^{k_z - 1}} + \sigma \frac{1 - \gamma}{\gamma^{k_z - 1}} \\ < -U_{\text{in}} - U_{\text{out}} \frac{1 - \gamma^{k_s}}{\gamma^{k_s}} + \sigma \frac{1 - \gamma}{\gamma^{k_s}}. \end{aligned} \quad (31)$$

We will show that (31) can be rewritten as (19). Then, recalling that  $\gamma \in [0, 1]$ ,  $\Delta_{\text{in}}, \Delta_{\text{out}} \geq 0$  and  $k_z \leq k_s$ , it is clear that (19) is stricter than (18) in Lemma III.13 (and thus implies it), hence proving the thesis that all Assumptions III.1, III.4, III.6, III.9 are compatible.

To show that (31) can be rewritten as (19), rewrite (31) as

$$\sigma > \frac{\gamma^{k_s} \gamma^{k_z-1} \Delta_{in}}{(1-\gamma)(\gamma^{k_z-1} - \gamma^{k_s})} + \frac{\gamma^{k_z-1}(1-\gamma^{k_s})U_{out}}{(1-\gamma)(\gamma^{k_z-1} - \gamma^{k_s})} - \frac{\gamma^{k_s}(1-\gamma^{k_z-1})L_{out}}{(1-\gamma)(\gamma^{k_z-1} - \gamma^{k_s})}. \quad (32)$$

Note that  $\gamma^{k_z-1}(1-\gamma^{k_s}) = (\gamma^{k_z-1} - \gamma^{k_s}) + \gamma^{k_s}(1-\gamma^{k_z-1})$ . Hence, we have

$$\frac{\gamma^{k_z-1}(1-\gamma^{k_s})U_{out}}{(1-\gamma)(\gamma^{k_z-1} - \gamma^{k_s})} = \frac{U_{out}}{1-\gamma} + \frac{\gamma^{k_s}(1-\gamma^{k_z-1})U_{out}}{(1-\gamma)(\gamma^{k_z-1} - \gamma^{k_s})},$$

and we rewrite (32) as

$$\sigma > \frac{\gamma^{k_s} \gamma^{k_z-1} \Delta_{in}}{(1-\gamma)(\gamma^{k_z-1} - \gamma^{k_s})} + \frac{U_{out}}{1-\gamma} - \frac{\gamma^{k_s}(1-\gamma^{k_z-1})\Delta_{out}}{(1-\gamma)(\gamma^{k_z-1} - \gamma^{k_s})}. \quad (33)$$

Now, note that

$$\frac{\gamma^{k_z-1}}{\gamma^{k_z-1} - \gamma^{k_s}} = \frac{\gamma^{k_z-1}(1-\gamma^{k_s}) - (\gamma^{k_z-1} - \gamma^{k_s})}{(\gamma^{k_z-1} - \gamma^{k_s})(1-\gamma^{k_s})} + \frac{1}{1-\gamma^{k_s}} = \frac{\gamma^{k_s}(1-\gamma^{k_z-1})}{(\gamma^{k_z-1} - \gamma^{k_s})(1-\gamma^{k_s})} + \frac{1}{1-\gamma^{k_s}},$$

and rewrite (33) as

$$\sigma > \frac{\gamma^{k_s}}{(1-\gamma)(1-\gamma^{k_s})} \Delta_{in} + \frac{U_{out}}{1-\gamma} + \frac{\gamma^{2k_s}(1-\gamma^{k_z-1})\Delta_{in}}{(1-\gamma)(\gamma^{k_z-1} - \gamma^{k_s})(1-\gamma^{k_s})} + \frac{\gamma^{k_s}(1-\gamma^{k_z-1})\Delta_{out}}{(1-\gamma)(\gamma^{k_z-1} - \gamma^{k_s})},$$

which is immediate to rewrite as (19).  $\square$

**Lemma A.2.** *Given two scalars  $a, b \in \mathbb{R}$ , with  $b \neq 0$ , if  $|a - b| < |b|$ , then  $\text{sign}(a) = \text{sign}(b)$ .*

*Proof.* We analyze separately the cases given by the combinations of the signs on  $a - b$  and  $b$ . (a) Let  $b > 0$ ,  $a - b \geq 0$ ; we have  $a \geq b > 0$ , that is  $a > 0$ . (b) Let  $b > 0$ ,  $a - b < 0$ ; we have  $-(a - b) < b$ , which simplifies to  $a > 0$ . (c) Let  $b < 0$ ,  $a - b \geq 0$ ; we have  $a - b < -b$  and thus  $a < 0$ . (d) Let  $b < 0$ ,  $a - b < 0$ ; we have  $a < b < 0$ , that is  $a < 0$ .  $\square$



**Francesco De Lellis** obtained his Ph.D. in Information Technology and Electrical Engineering at the University of Naples Federico II in May 2023. He has been a visiting researcher at the University College Dublin in 2020 and the University College London in 2022. Today, Francesco is a postdoctoral fellow with the University of Napoli Federico II. The core of Francesco's research deals with the application of control theory, reinforcement learning and supervised learning for the development of new methodologies for the control of multi-agent complex systems.

plex systems.



**Marco Coraggio** (Member, IEEE) received the Ph.D. degree in information technology and electrical engineering from the University of Naples Federico II, Naples, Italy, in 2020. He was a Postdoctoral Fellow with the University of Naples Federico II from 2020 to 2021 and has been a Postdoctoral Fellow with the Scuola Superiore Meridionale, School for Advanced Studies, Naples, since 2021. He was a Visiting Student with the University of Bristol, Bristol, U.K., in 2016, a Visiting Scholar at the University of California, Santa Barbara, CA, USA, in 2019, and at the Linköping University, Linköping, Sweden, in 2023. He was the finalist, in 2022, and the winner, in 2023, of the IEEE CSS Italy Young Author Best Paper Award. His current research interests include complex networks and applications, data-driven control, and piecewise smooth and hybrid dynamical systems.



**Giovanni Russo** (Senior Member, IEEE) is an Associate Professor of Automatic Control at the University of Salerno, Italy. He was previously with the University of Naples Federico II (Ph.D. in 2010), Italy, Ansaldo STS (System Engineer/Integrator of the Honolulu Rail Transit Project, USA in 2012-2015), IBM Research Ireland (Research Staff Member in Optimization, Control and Decision Science from 2015 to 2018) and University College Dublin, Ireland (in 2018-2020). His research interests include contraction theory, analysis/control of nonlinear and complex systems, data-driven sequential decision-making under uncertainty and control in the space of densities. Dr. Russo has served as Associate Editor for the IEEE Transactions on Circuits and Systems I: regular papers (2016-2019) and the IEEE Transactions on Control of Network Systems (2017-2023). Since January 2024, Dr. Russo is serving as Senior Editor for the IEEE Transactions on Control of Network Systems. Personal page: <https://tinyurl.com/2p8zfpme>.



**Mirco Musolesi** is Full Professor of Computer Science at the Department of Computer Science at University College London, where he leads the Machine Intelligence Lab, as part of the Autonomous Systems Research Group. He is also Full Professor of Computer Science at the University of Bologna. Previously, he held research and teaching positions at Dartmouth, Cambridge, St Andrews and Birmingham. He has broad research interests spanning several traditional and emerging areas of Computer Science and beyond. The focus of his lab is on machine learning/artificial intelligence and their applications to a variety of theoretical and practical problems and domains. More information about his profile can be found at: <https://www.mircomusolesi.org>



**Mario di Bernardo** (Fellow, IEEE) is Professor of Automatic Control at the University of Naples Federico II, Italy and Visiting Professor of Nonlinear Systems and Control at the University of Bristol, U.K. He currently serves as Deputy pro-Vice Chancellor for Internationalization at the University of Naples and coordinates the research area and PhD program on Modeling and Engineering Risk and Complexity of the Scuola Superiore Meridionale located in Naples. On 28th February 2007 he was bestowed the title of Cavaliere of the Order of Merit

of the Italian Republic for scientific merits from the President of Italy. He was elevated to the grade of Fellow of the IEEE in January 2012 for his contributions to the analysis, control and applications of nonlinear systems and complex networks. He was President of the Italian Society for Chaos and Complexity (2010-2017), member of the Board of Governors (2006-2011) and Vice President for Financial Activities (2011-2014) of the IEEE Circuits and Systems Society. In 2015 he was appointed to the Board of Governors of the IEEE Control Systems Society where he was elected member for the term 2023-2025. He was Distinguished Lecturer of the IEEE Circuits and Systems Society (2016-2017). He authored or co-authored more than 220 international scientific publications including more than 150 papers in scientific journals, a research monograph and two edited books. According to the international database SCOPUS (September 2023), his h-index is 53 and his publications received over 12000 citations by other authors. In 2017, he received the IEEE George N. Saridis Best Transactions Paper Award for Outstanding Research. He was Deputy Editor-in-Chief of the IEEE Transactions on Circuits and Systems: Regular Papers, Senior Editor of the IEEE Transactions on Control of Network Systems and Associate Editor of the IEEE Control Systems Letters, Nonlinear Analysis: Hybrid Systems, the IEEE Transactions on Circuits and Systems I, and the IEEE Transactions on Circuits and Systems II. He is regularly invited as Plenary Speaker in Italy and abroad. He has been organizer and co-organizer of several scientific initiatives and events and received funding from several funding agencies and industry including the European Union, the UK research councils the Italian Ministry of Research and University.